RADIATION HARD SEMICONDUCTOR DEVICES FOR VERY HIGH LUMINOSITY COLLIDERS

Development of radiation tolerant Silicon Sensors - A Status Report of the RD50 Collaboration -

Marta Baselga Bacardit
CNM-IMB, CSIC Barcelona
On behalf of the RD50 collaboration

Outline

- The RD50 Collaboration
  - An overview of RD50 achievements
- New Projects
  - Defects and material characterization
  - Detector characterization
  - New structures
  - Full detector systems
- Summary

Motivation

- New LHC upgrades silicon detectors will receive fluences up to 2e16n_{eq}/cm^2 (expected luminosity: 3000fb^{-1})

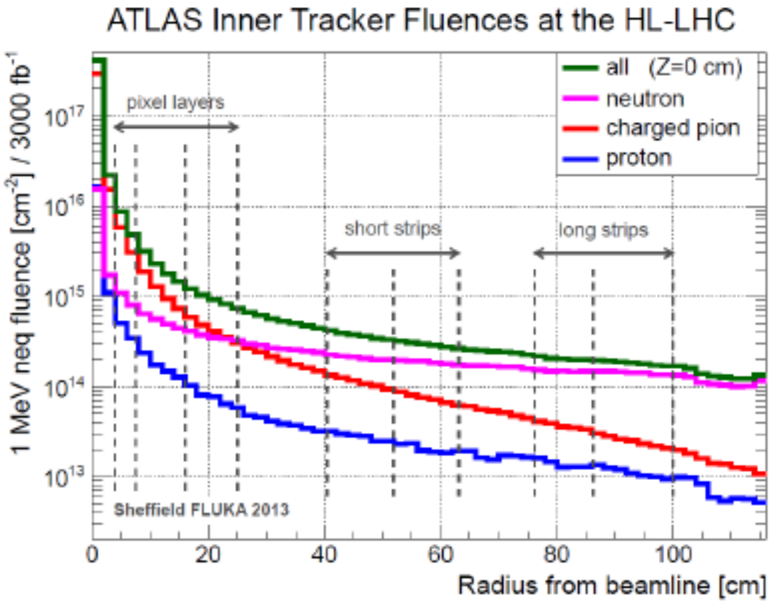

[I. Dawson, P. S. Miyagawa, Sheffield University, Atlas Upgrade radiation background simulations]

- RD50 is a R&D collaboration that wants to develop radiation hard semiconductor devices for very high luminosity colliders

The RD50 Collaboration

- RD50: 49 *institutes and 280 members*

41 European institutes

Belarus (Minsk), Belgium (Louvain), Czech Republic (Prague (3x)), Finland (Helsinki, Lappeenranta), France (Paris, Orsay), Germany (Dortmund, Erfurt, Freiburg, Hamburg (2x), Karlsruhe, Munich(2x)), Italy (Bari, Florence, Perugia, Pisa, Torino), Lithuania (Vilnius), Netherlands (NIKHEF), Poland (Krakow, Warsaw(2x)), Romania (Bucharest (2x)), Russia (Moscow, St.Petersburg), Slovenia (Ljubljana), Spain (Barcelona(2x), Santander, Valencia), Switzerland (CERN, PSI), Ukraine (Kiev), United Kingdom (Glasgow, Liverpool)

6 North-American institutes

Canada (Montreal), USA (BNL, Fermilab, New Mexico, Santa Cruz, Syracuse)

1 Middle East institute

Israel (Tel Aviv)

1 Asian institute

India (Delhi)

Detailed member list: http://cern.ch/rd50

RD50 Organizational Structure

Co-Spokespersons

Gianluigi Casse **and** ***Michael Moll***

(Liverpool University) (CERN PH-DT)

Defect / Material Characterization

Ioana Pintilie
(NIMP Bucharest)

- **Characterization of microscopic properties of standard-, defect engineered and new materials pre- and post- irradiation**
- **DLTS, TSC, ….**
- **SIMS, SR, …**
- **NIEL (calculations)**
- WODEAN: Workshop on Defect Analysis in Silicon Detectors (G.Lindstroem & M.Bruzzi)

Detector Characterization

Eckhart Fretwurst
(Hamburg University)

- **Characterization of test structures (IV, CV, CCE, TCT,.)**
- **Development and testing of defect engineered silicon devices**
- **EPI, MCZ and other materials**
- **NIEL (experimental)**
- **Device modeling**
- **Operational conditions**
- **Common irradiations**
- Wafer procurement (M.Moll)
- Device Simulations (V.Eremin)

New Structures

Giulio Pellegrini
(CNM Barcelona)

- **3D detectors**
- **Thin detectors**
- **Cost effective solutions**
- **Detectors with internal gain (avalanche detectors LGAD)**
- **Slim Edges**
- **Other new structures**

- 3D (R.Bates)
- LGAD (V. Greco)
- Slim Edges (V. Fadeyev)

Full Detector Systems

Gregor Kramberger
(Ljubljana University)

- **LHC-like tests**
- **Links to HEP**
- **Links electronics R&D**
- **Low rho strips**
- **Sensor readout (Alibava)**
- **Comparison:**
  - **pad-mini-full detectors**
  - **different producers**
- **Radiation Damage in HEP detectors**

- Test beams (M. Bomben & G.Casse)

Collaboration Board Chair & Deputy: G.Kramberger (Ljubljana) & J.Vaitkus (Vilnius), Conference committee: U.Parzefall (Freiburg)
CERN contact: M.Moll (PH-DT), Secretary: V.Wedlake (PH-DT), Budget holder & GLIMOS: M.Glaser (PH-DT)

Defects reminders

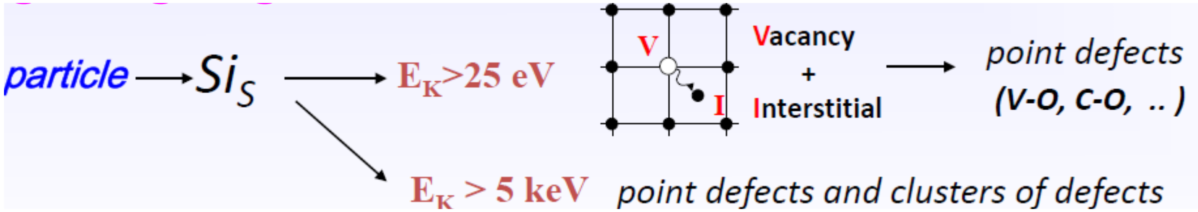

Defects generation depends on the type of the particles and energy, thus it is scaled at 1 MeV neutron equivalent (NIEL Hypothesis).

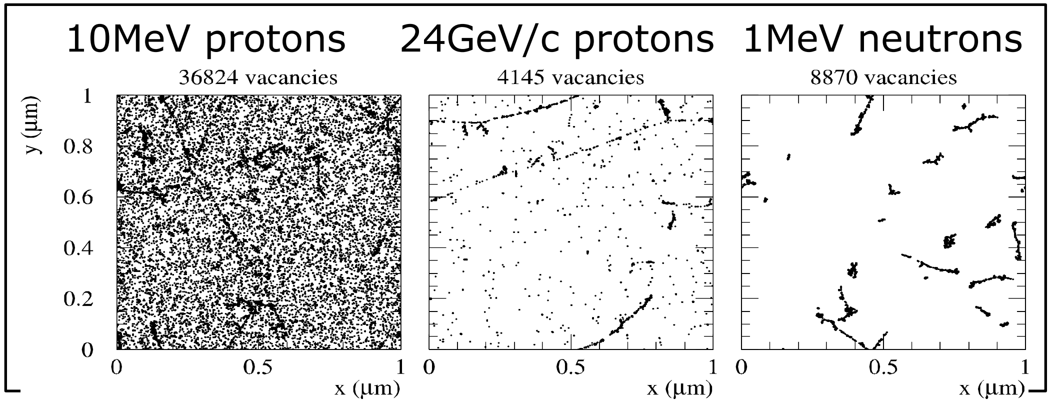

[Mika Huhtinen NIMA 491(2002) 194]

Simulation with initial distribution of vacancies in $(1\text{um})^3$ after 10^{14} particles/cm^3

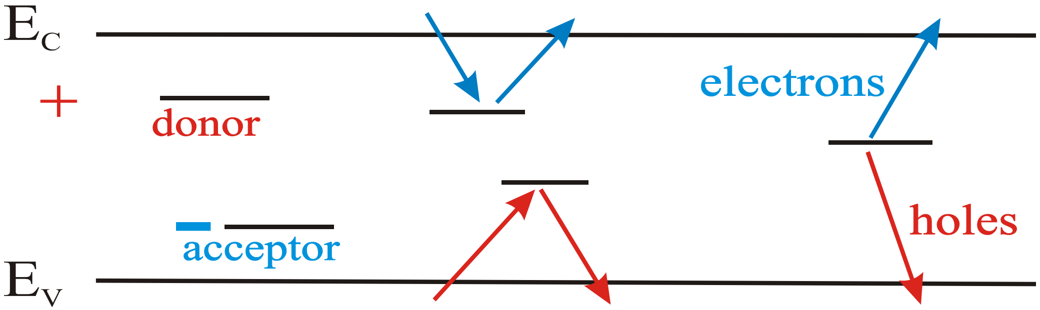

charged → Space Charge, E-Field

capture e or h → trapping

generation e,h → leakage current

Microscopic defects change characteristics in the macroscopic scale

Defect

- Defect characterization
  - Identify defects responsible for Trapping, Leakage Current, Change of N_{eff} , Change of E-Field
  - Understand them and mitigate the radiation damage
- Macroscopic observations:
  - Neutron irradiated materials leads to net negative space charge
  - Hadron irradiation leads to build up of net positive space charge

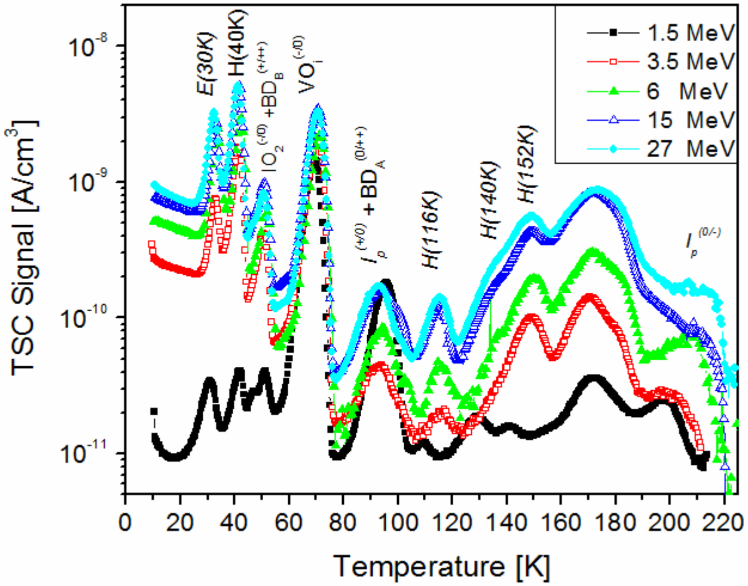

[R.Radu et al, J. Appl. Physics 117, 164503, 2015]

TSC measurement produced by electron irradiation (1.5 to 27 MeV)

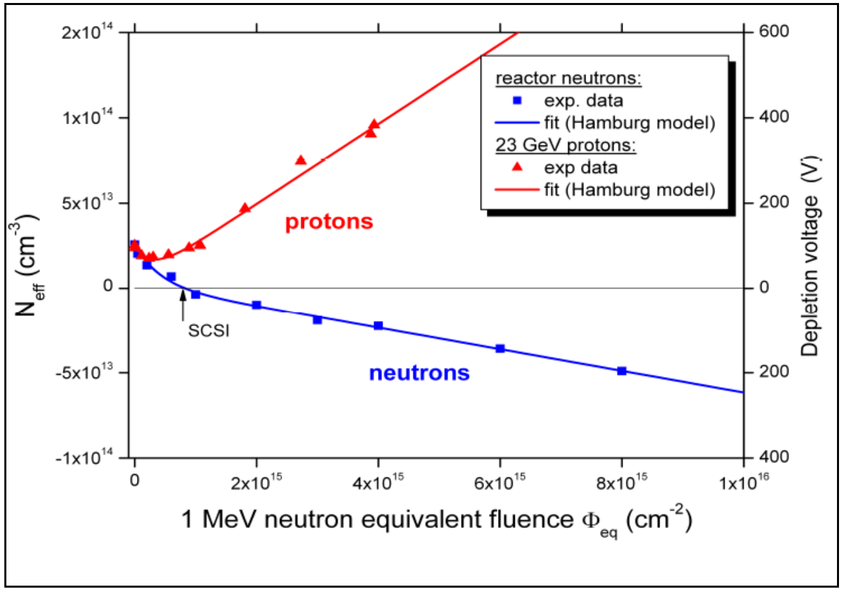

[I. Pintilie et al, Nucl. Instr. And Meth. A 611, 52-68, (2009)]

Defects with strong impact on device performance after irradiation

M. Moll, RD50 Status Report, Vertex 2013

Phosphorus: shallow dopant (positive charge)

positive charge (higher introduction after proton than after neutron irradiation, oxygen dependent)

[I. Pintilie et al, Nucl. Instr. and Meth. A **514**, 18 (2003) and Nucl. Instr. and Meth. A **556**, (1), 197 (2006); E. Fretwurst et al, Nucl. Instr. and Meth. A **583**, 58 (2007)]

positive charge (higher introduction after proton irradiation than after neutron irradiation)

[I. Pintilie et al, Nucl. Instr. And Meth. A 611, 52-68, (2009)]

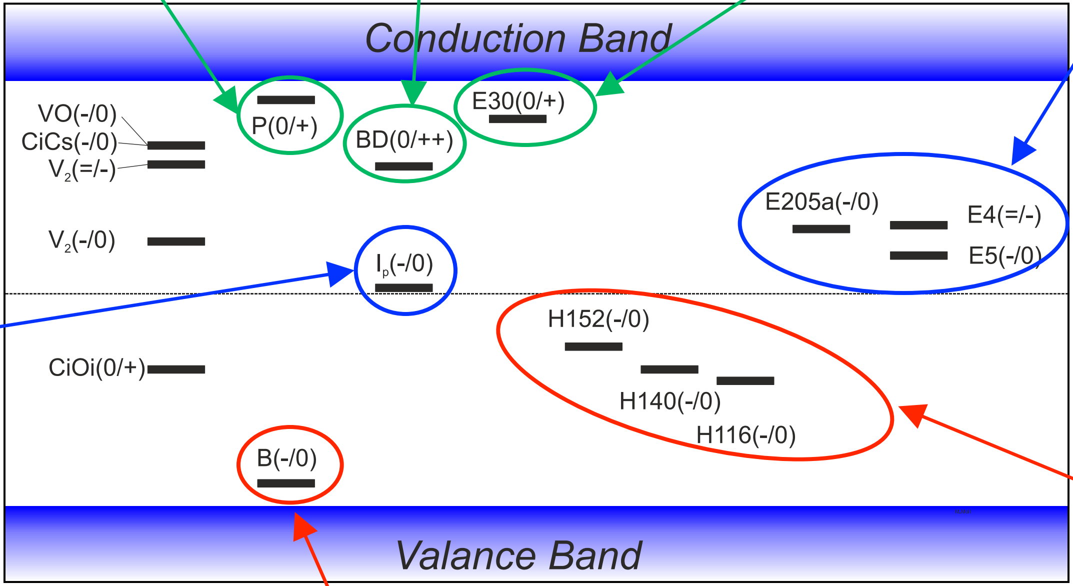

Leakage current

E4/E5: V_3 (?)

[R. M. Fleming, et al Appl. Phys. Lett. **90**, 172105 (2007) ; V. P. Markevich, et al Phys. Rev. B **80**, 235207 (2009); A. Junkes et al, Nucl. Instr. and Meth. A **525**, 612 (2010)]

leakage current & neg. charge

current after γ irrad, V_2O (?)

[I. Pintilie et al, Appl.Phys. Lett.**82**, 2169 (2003)]

Reverse annealing

(negative charge)

[I. Pintilie et al, Appl. Phys. Lett. **92**, 024101 (2008)]

Boron: shallow dopant (negative charge)

*Software simulations for defects seen in Timo Peltola presentation

Choice of silicon sensors for segmented detectors

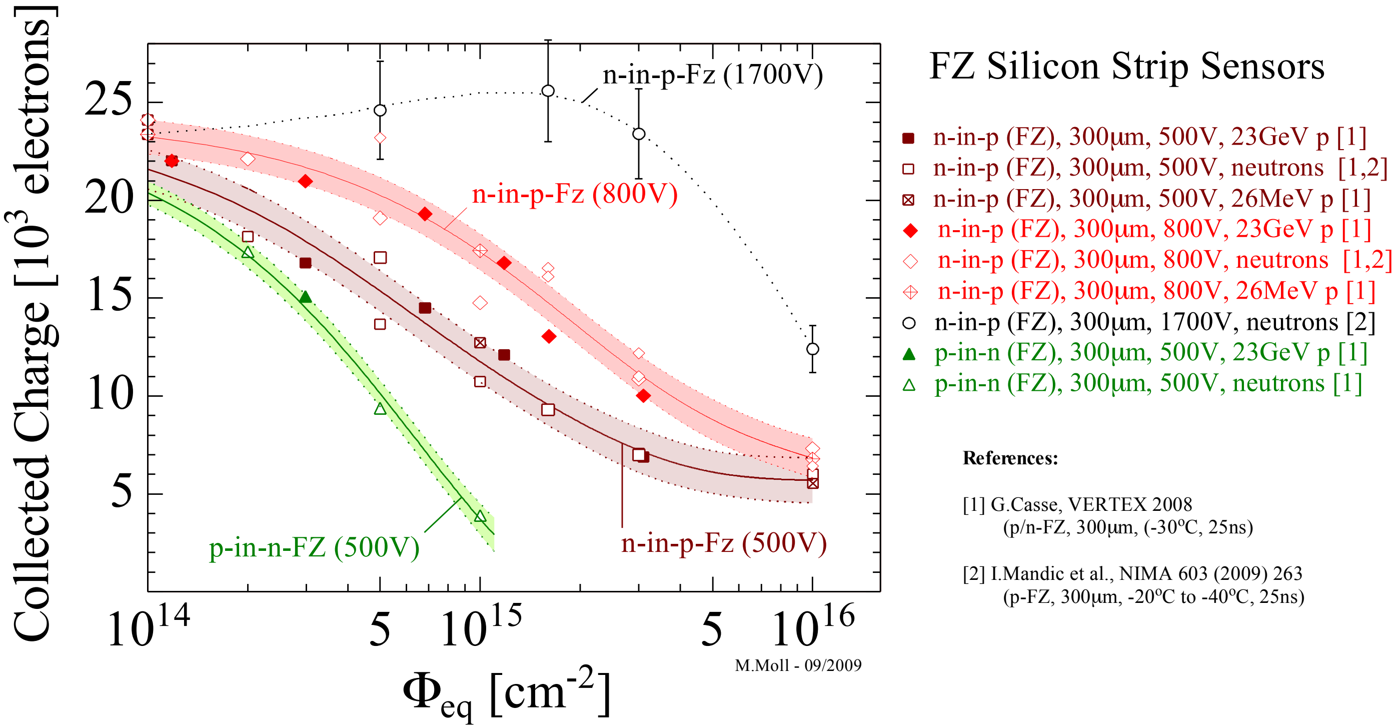

References:

[1] G.Casse, VERTEX 2008
(p/n-FZ, 300µm, (-30°C, 25ns)

[2] I.Mandic et al., NIMA 603 (2009) 263
(p-FZ, 300µm, -20°C to -40°C, 25ns)

- Choice of p-type silicon for RD50, now used at ATLAS and CMS
- Electric field and weighting field are maximum at the same electrode
- Electron collection:
  - Faster mobility
  - Electrons can multiply
  - Decrease of trapping probability after annealing for electrons

FZ n-in-p microstrip detector

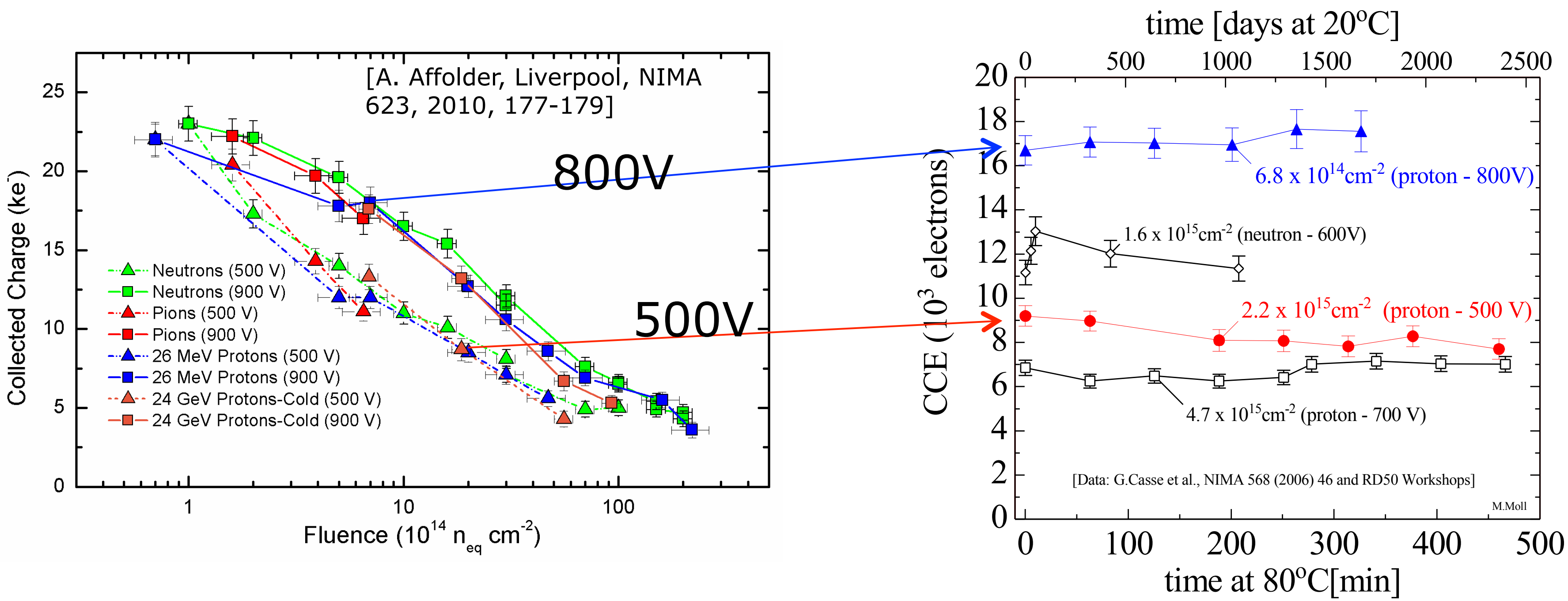
[A. Affolder, Liverpool, NIMA 623, 2010, 177-179]

[Data: G.Casse et al., NIMA 568 (2006) 46 and RD50 Workshops]

M.Moll

No reverse annealing in CCE measurements for neutron and proton irradiated detectors

Charge multiplitcation after irradiation

Strips 26MeV protons, Alibava measurements

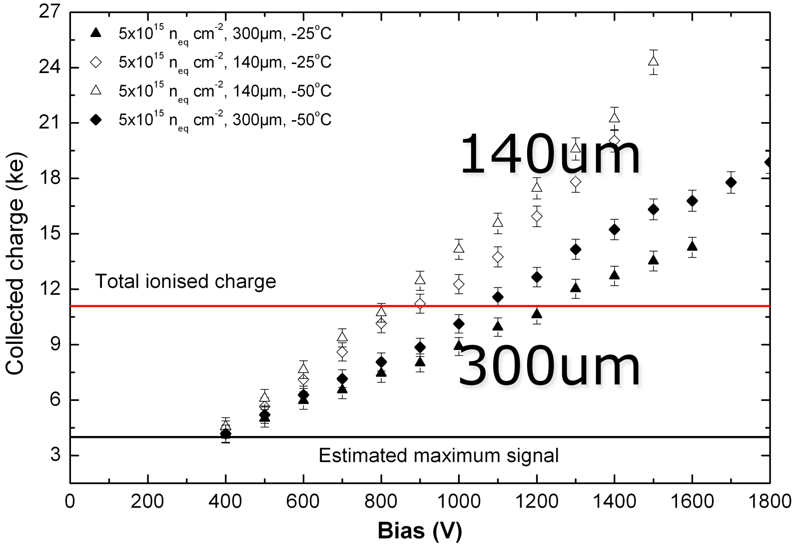

G. Casse NIMA 624 (2010) pp. 401-404

3D

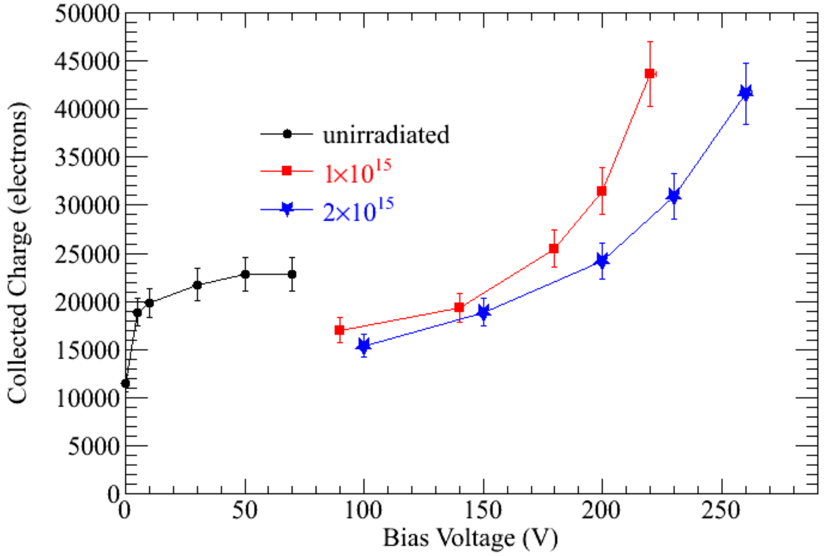

M. Köhler, NIMA 659 (2011) 272-281

Space charge after irradiation ($\Phi\geq10^{15}n_{eq}/cm^2$) leads to high electric field near the electrodes

3D sensors (Φ_{eq}=1-2×10^{15} cm^{-2}) Charge Collection (test beam)

NEW PROJECTS

Defects and material characterization

- Nitrogen doping float zone -> Nitrogen enriched float zone silicon for high energy particle detectors
  - NitroSil project on vacancy aggregation in silicon single crystals

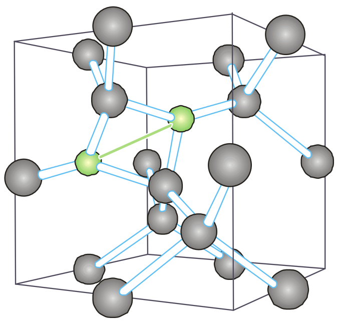

N_iN_i dimer
two split-interstitials

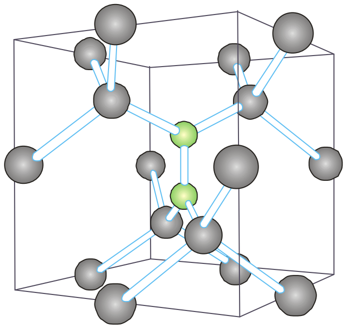

N_iN_s pair
N_s + split-interstitial

- R. Jones *et all*. Solid State Phenomena 93, (2004) 95-96

In particular, the concentrations of radiation centers with the activation energies of 30 meV, 310 meV, 360 meV, 380 meV, and 460 meV are found to be significantly lower in the material with a higher nitrogen concentration.

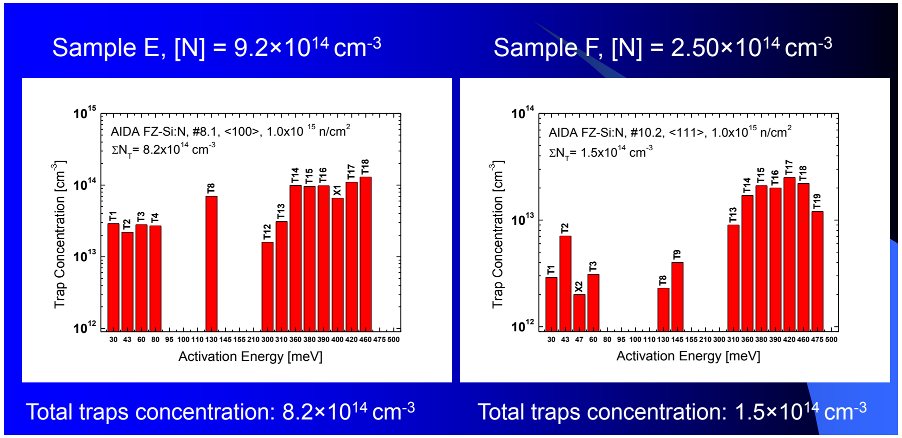

Sample E, [N] = 9.2×10^{14} cm^{-3}

Sample F, [N] = 2.50×10^{14} cm^{-3}

Total traps concentration: 8.2×10^{14} cm^{-3}

Total traps concentration: 1.5×10^{14} cm^{-3}

Fluence: $1x10^{15}n_{eq}/cm^3$

[Vaitkus RD50 Workshop, November 2014]

HVCMOS characterization

- The charge collection mechanism is a drift in a thin depletion region (10-20um).
- Depleted active implemented in CMOS process
- Hit position encoded as the height of the pulse in the pixel line
- Strip and pixel possible geometry

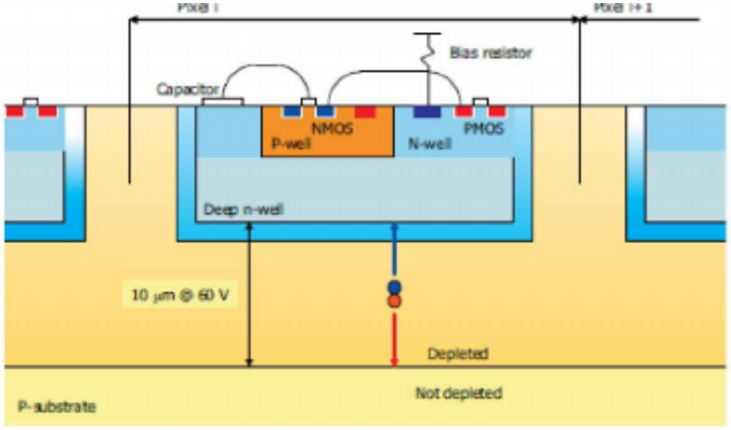

M. Fernandez, 25th RD50 Workshop, Nov. 2014

E-TCT measurements:

To understand charge collection properties

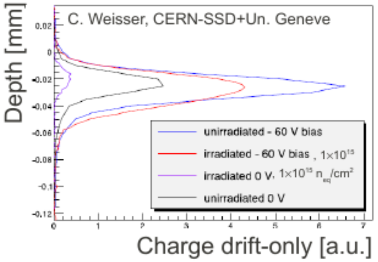

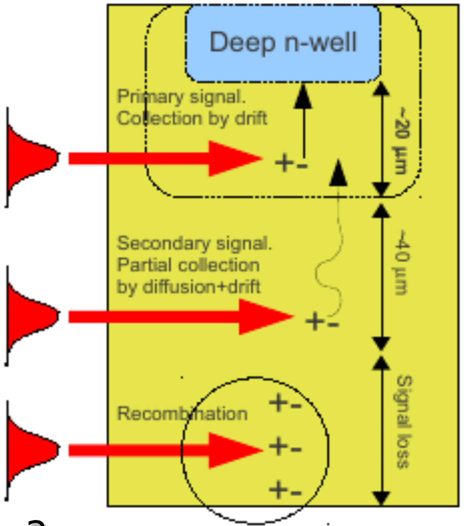

Side view of HVCMOS

Signal map for non-irradiated and irradiated HVCMOS

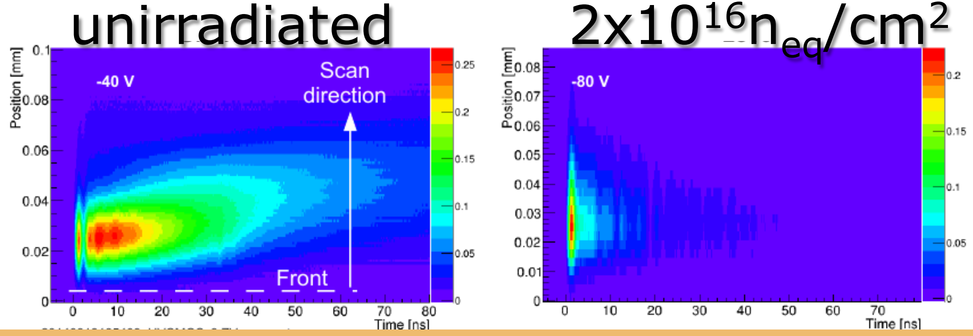

[M. Fernandez, 25th RD50 workshop, 2014]

Low Gain Avalanche Detectors: LGAD

High Electric Field region leading to multiplication

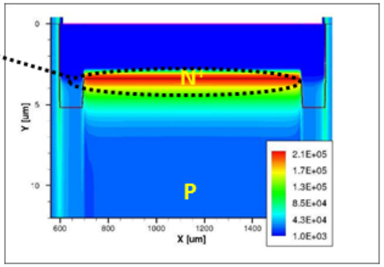

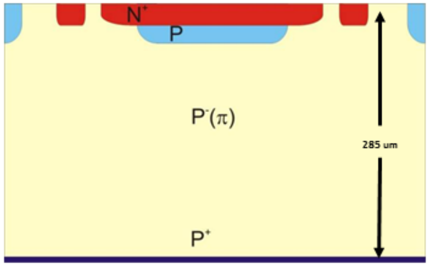

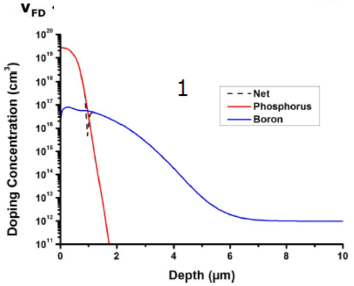

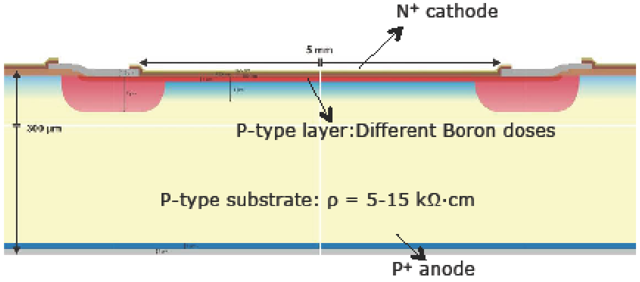

$V_{FD} < 30$ V

$V_{BD} > 1100$ V

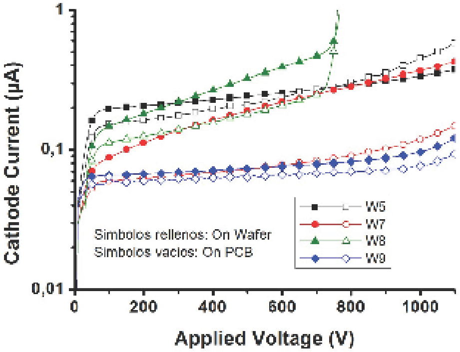

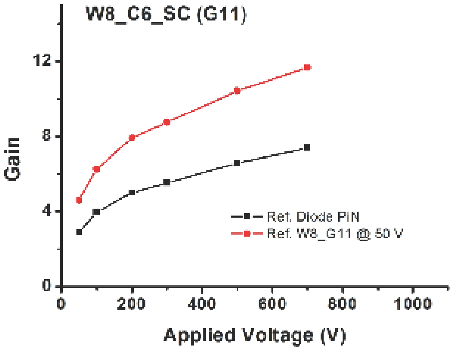

[G. Pellegrini, NIMA 765 (2014) pp. 12-16]

TCT measurement with alpha particles with and without gain

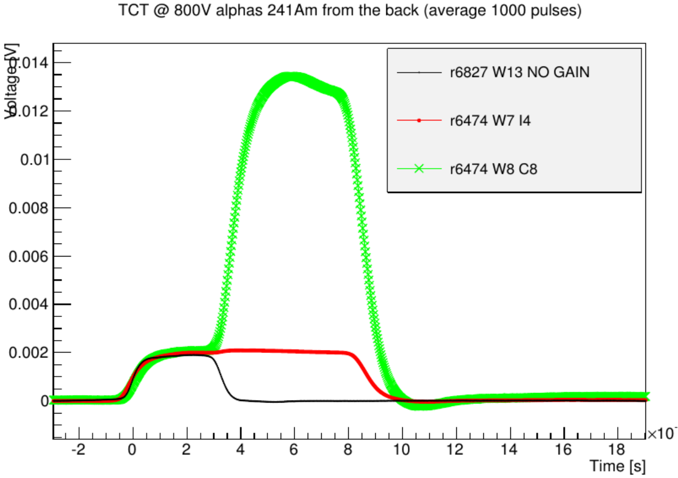

[H. Sadrozinski NIMA 765 (2014) pp. 7-11]

CM after irradiation for LGAD

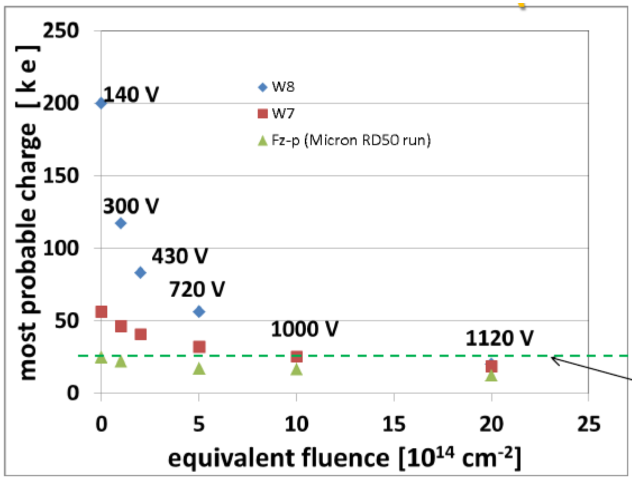

$$M_Q = \frac{Q_{W7,W8}}{Q_{st.diode}}$$

Neutrons

~25000 e
(st. nirr. diode)

M_Q~1.5

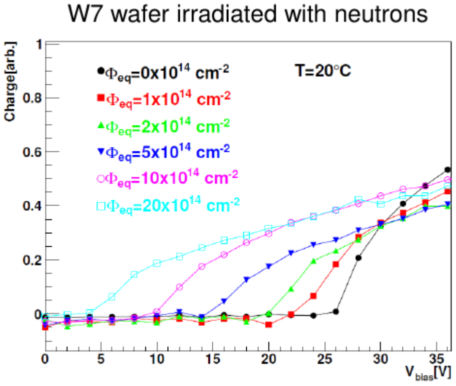

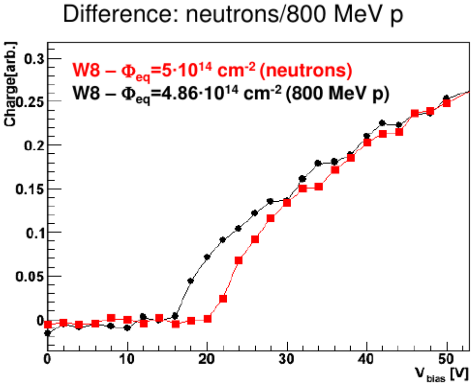

[G. Kramberger in 24th RD50 workshop june 2014]

Multiplication is reduced after irradiation-> seems like the boron is removed after irradiation

Ultra Fast silicon Detectors: UFSD

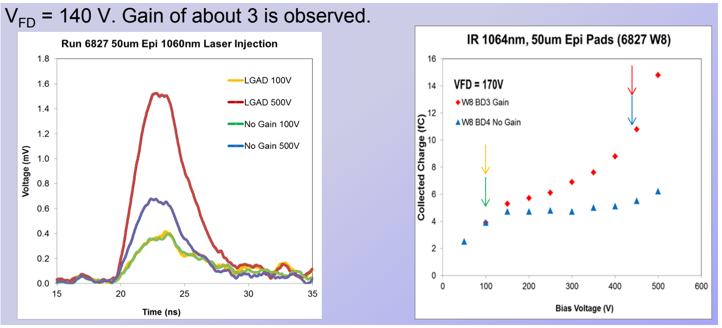

V_{FD} = 140 V. Gain of about 3 is observed.

Thin sensors give:
-Faster signal
-Precision location information

[H. Sadrozinski, 25th RD50 workshop, november 2014]

Segmented LGAD & UFSD: RD50 Project

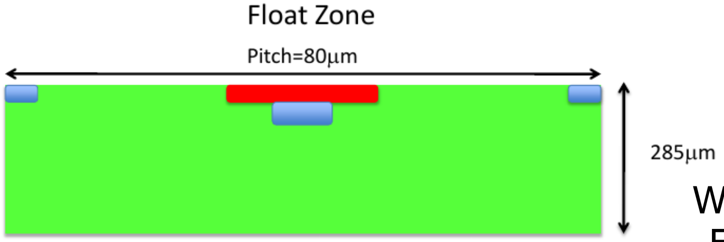

Wafers:
-FZ
-10um epitaxial
-50um epitaxial
-75um epitaxial

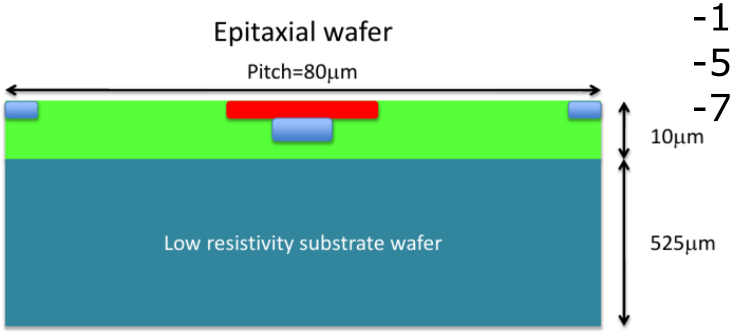

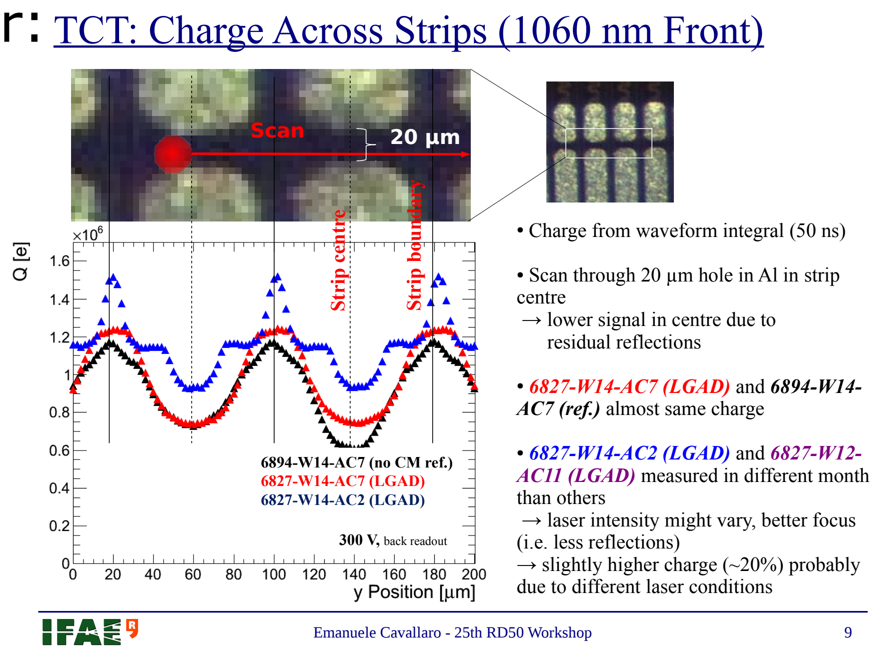

FZ wafer: TCT: Charge Across Strips (1060 nm Front)

- Charge from waveform integral (50 ns)
- Scan through 20 µm hole in Al in strip centre
  → lower signal in centre due to residual reflections
- *6827-W14-AC7 (LGAD)* and *6894-W14-AC7 (ref.)* almost same charge
- *6827-W14-AC2 (LGAD)* and *6827-W12-AC11 (LGAD)* measured in different month than others
  → laser intensity might vary, better focus (i.e. less reflections)
  → slightly higher charge (~20%) probably due to different laser conditions

IFAE Emanuele Cavallaro - 25th RD50 Workshop 9

R6827W14AC11 FZ Deep gain

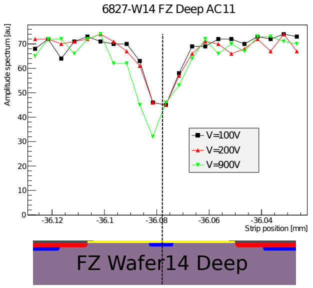

Data from 10^5 events

R6827W13DC1 FZ Standard gain

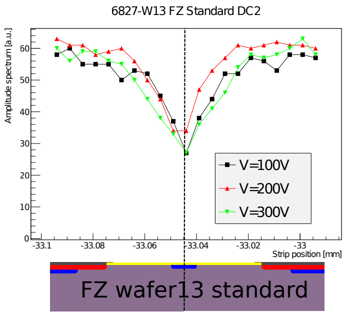

Data from 10^5 events

IBIC Sevilla: R6827W14AC4 FZ Deep protons 2MeV 400V

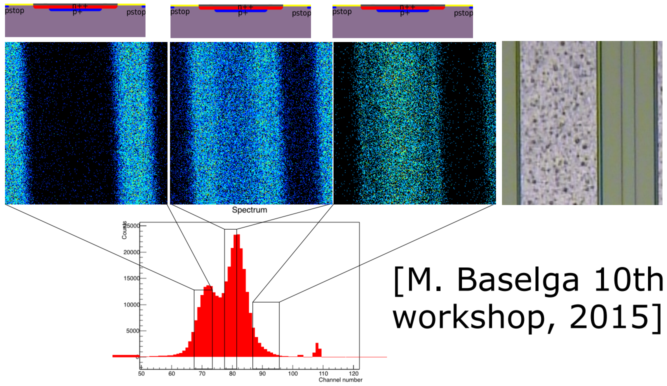

[M. Baselga 10th Trento workshop, 2015]

Diamond light source photons at 15keV

3D developed for IBL and for new upgrade:

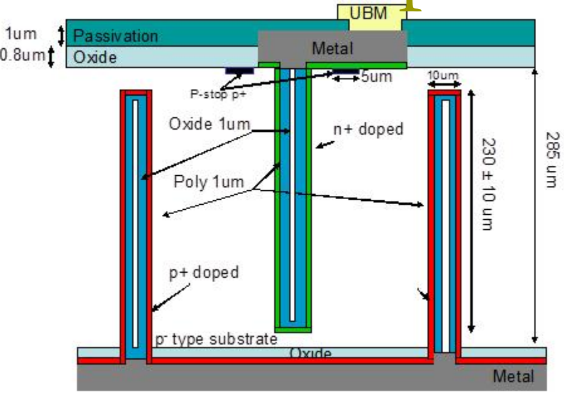

[G. Pellegrini, NIMA 592 (2008) 38-43]

C: 50x50um² with the rest connected to GND with 3DGR

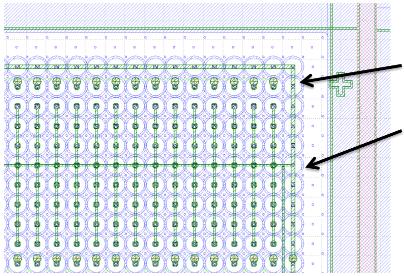

P-stop width 5um
Internal radii 22.5um

Pixels connected to ground

B: 25x100um2 ("25x500" 1E, with 3DGR)

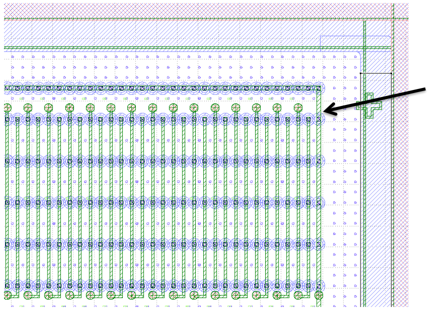

P-stop width 5um
Internal radii 10um

Pixel cell 25x100 um
(total length 500um).

Increasing aspect ratio @ CNM:
Cryogenic Silicon DRIE

Pulsed process:

Etching gas: SF_6

~~*Sidewall passivation: C_4F_8*~~

Possibility to achieve ***higher*** *aspect ratio (up to 40:1)*

Not with cryogenic

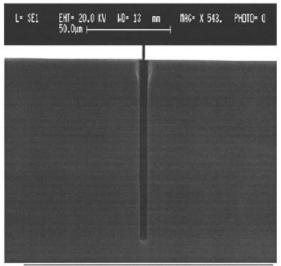

FIG. 11. Cross-sectional SEM image of silicon etch by using helicon reactor with cryogenic process (1999).

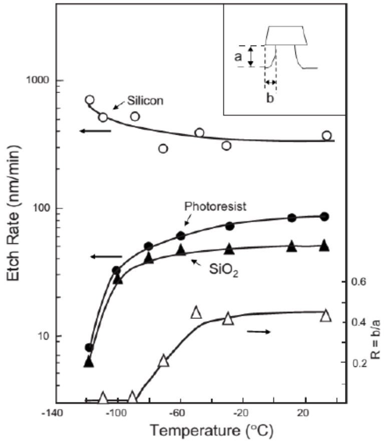

FIG. 10. Etch properties at cryogenic processes.

B. Wu et al., J. App. Phys. 108 (2010) 051101

MIP Simulation:

50umx50umx200um **100umx25umx200um**

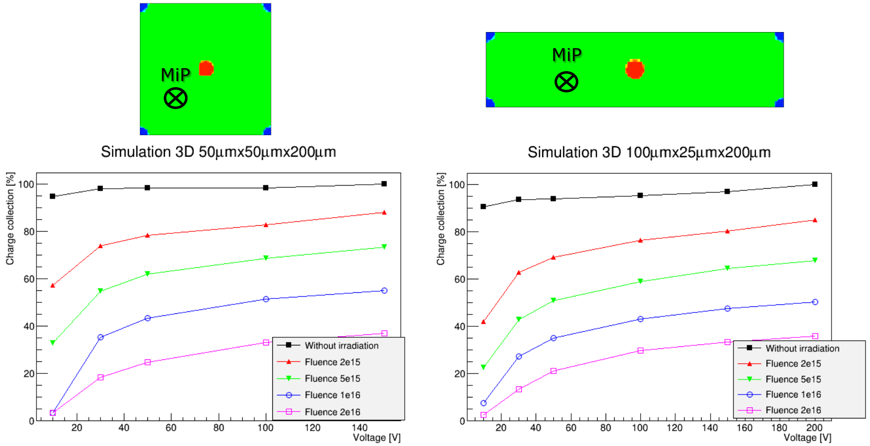

[M. Baselga, 10th Trento workshop, 2015]

*More details for 3D detectors were presented in Jörn Lange talk

New irradiation facility at CERN

- New PS east area irradiation facilities
  - IRRAD proton facility
  - CHARM Mixed-Field Facility

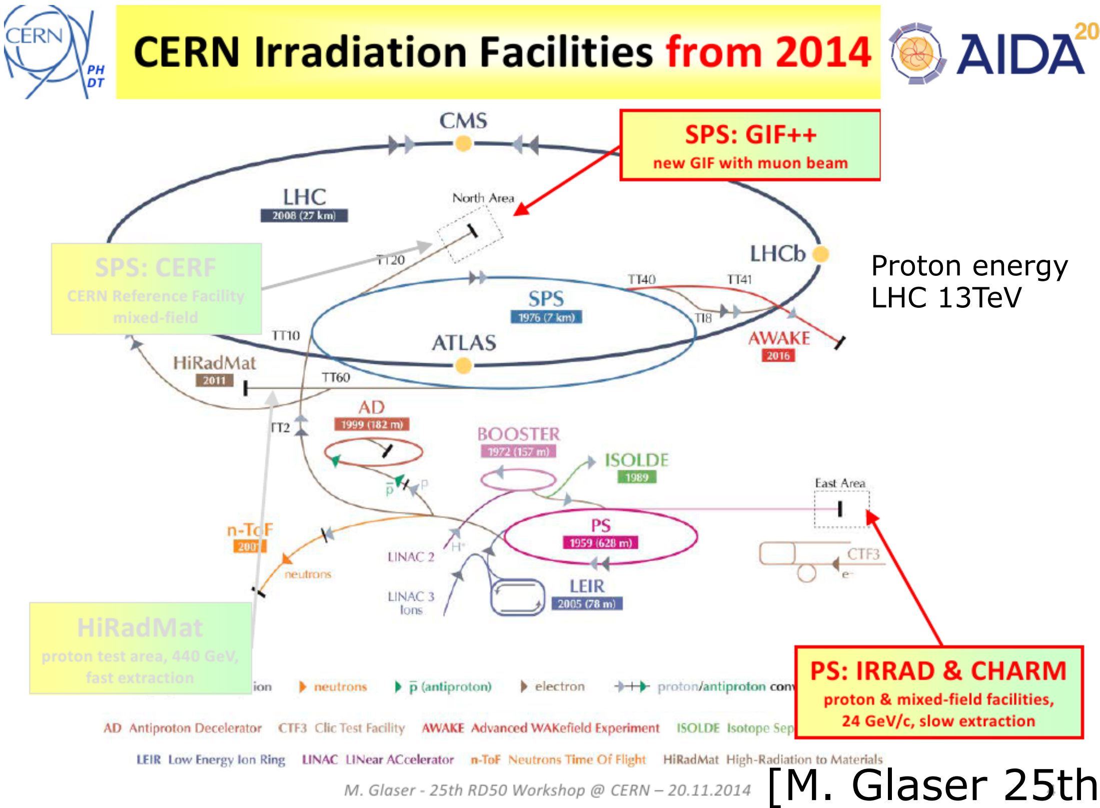

CERN Irradiation Facilities from 2014

SPS: GIF++
new GIF with muon beam

SPS: CERF
CERN Reference Facility
mixed-field

HiRadMat
proton test area, 440 GeV,
fast extraction

PS: IRRAD & CHARM
proton & mixed-field facilities,
24 GeV/c, slow extraction

M. Glaser - 25th RD50 Workshop @ CERN – 20.11.2014

Proton energy
LHC 13TeV

Proton irradiation
Beam spot 12x12mm^2
Momentum: 24GeV/c
Proton flux: 10^{16}pcm^{-2} 5days^{-1}

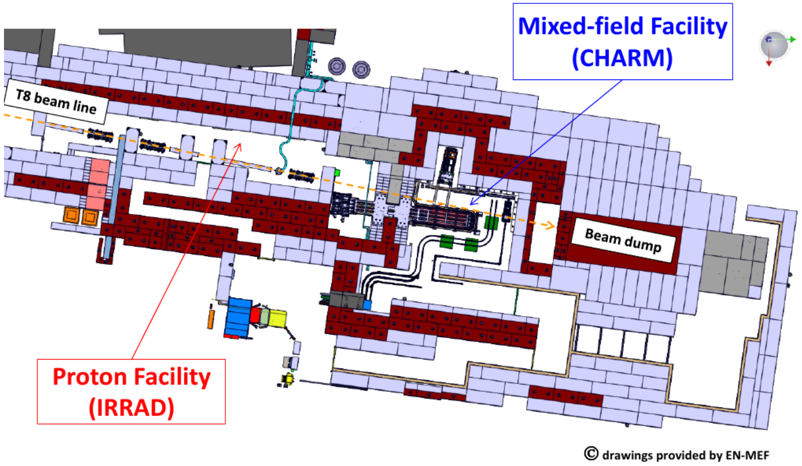

© drawings provided by EN-MEF

[M. Glaser 25th RD50 Workshop – november 2014]

Summary

- RD50 is a CERN collaboration for **Radiation hard semiconductor devices for very high luminosity colliders**
- Most activity is focused on Silicon detectors for future collider experiments
- Different blocks of the collaboration:
  - Defects and material characterization: Detailed understanding of microscopic defects, consistent list of defects
  - Detector characterization: TCT, E-TCT measurements, parallel strip measurement
  - Device simulation: Simulation results, common database
  - Full detector system: Charge multiplication effect systematically investigated to allow its explotation
  - New structures:
    - Slim/active edges: Production controlled and pixel close to edge highly efficient
    - 3D-detectors, performing in IBL
    - HVCMOS: Few samples tested, drift signal changes barely after irradiation, diffusion signal and trapping reduce charge (50% charge after $2 \cdot 10^{16} n_{eq}/cm^2$)
    - LGAD: uniform gain up to 20 before irradiation, decrease after irradiation
    - Thin, low-R strip sensors, …

Thanks for your attention

More details on:

http://rd50.web.cern.ch/rd50/

BACKUP

Relevant defects

TABLE I. Electrical properties of point and extended defects relevant for detector operation.

Defect label	Assignment and particularities	Configurations and charge states	Energy levels (eV) and capture cross sections (cm^2)	Impact on electrical characteristics of Si diodes at RT
E(30 K)	Not identified extended defect. Donor with energy level in the upper part of the bandgap, strongly generated by irradiation with charged particles[10,29] Linear fluence dependence (this work)	$E(30\,K)^{0/+}$	$E_c - 0.1\ \sigma_n = 2.3 \times 10^{-14}$	Contributes in full concentration with positive space charge to N_{eff}
BD	*TDD2*—point defect Bistable donor existing in two configurations (A and B) with energy levels in the upper part of the bandgap, strongly generated in Oxygen rich material[24,26,27]	$BD_A{}^{0/++}$ $BD_B{}^{+/++}$	$E_C - 0.225\ \sigma_n = 2.3 \times 10^{-14}$ $E_C - 0.15\ \sigma_n = 2.7 \times 10^{-12}$	It contributes twice with its full concentration with positive space charge to N_{eff}, in both of the configurations
I_p	Not identified point defect. Suggestions: V_2O or a Carbon related center[10,22–24] Amphoteric defect generated via a second order process (quadratic fluence dependence), strongly generated in Oxygen lean material[22–24] (this work)	$I_p{}^{+/0}$ $I_p{}^{0/-}$	$E_V + 0.23\ \sigma_p = (0.5–9) \times 10^{-15}$ $E_C - 0.545\ \sigma_n = 1.7 \times 10^{-15}$ $\sigma_p = 9 \times 10^{-14}$	No impact Contributes to both N_{eff} and LC
E_{75} E4 E5	*Tri-vacancy (V_3)*—small cluster Bistable defect existing in two configurations (FFC and PHR) with acceptor energy levels in the upper part of the bandgap[10,28,30–33] Linear fluence dependence (this work)	$FFCV_3{}^{-/0}$ $PHRV_3{}^{=/-}$ $PHRV_3{}^{-/0}$	$E_c - 0.075\,eV\ \sigma_n = 3.7 \times 10^{-15}$ $E_c - 0.359\ \sigma_n = 2.15 \times 10^{-15}$ $E_c - 0.458\ \sigma_n = 2.4 \times 10^{-15}$ $\sigma_p = 2.15 \times 10^{-13}$	No impact No impact Contributes to LC
H(116 K)	Not identified extended defect. Acceptor with energy level in the lower part of the bandgap[10,29] Linear fluence dependence (this work)	$H(116\,K)^{0/-}$	$E_V + 0.33\ \sigma_p = 4 \times 10^{-14}$	Contributes in full concentration with negative space charge to N_{eff}
H(140 K)	Not identified extended defect. Acceptor with energy level in the lower part of the bandgap[10,29] Linear fluence dependence (this work)	$H(140\,K)^{0/-}$	$E_V + 0.36\ \sigma_p = 2.5 \times 10^{-15}$	Contributes in full concentration with negative space charge to N_{eff}
H(152 K)	Not identified extended defect. Acceptor with energy level in the lower part of the bandgap[10,29] Linear fluence dependence (this work)	$H(152\,K)^{0/-}$	$E_V + 0.42\ \sigma_p = 2.3 \times 10^{-14}$	Contributes in full concentration with negative space charge to N_{eff}

[R.Radu et al, J. Appl. Physics 117, 164503, 2015]

TCT-TPA: Transient Current Technique on Two Photon Absorption process

- TPA: transitions that may be impossible to excite with one photon it may be reachable with two photons
- Femto-second laser setup,

increases the probability TPA by 10^5

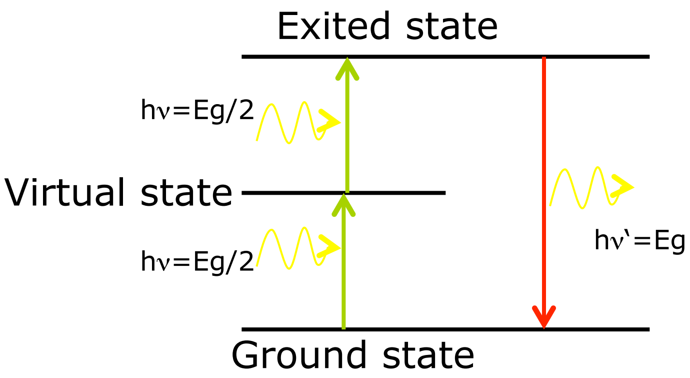

Exited state

hν=Eg/2

Virtual state

hν=Eg/2

hν'=Eg

Ground state

Good simulation agreement with data:

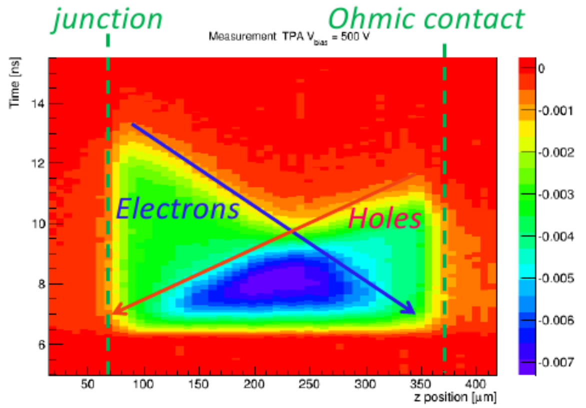

Data

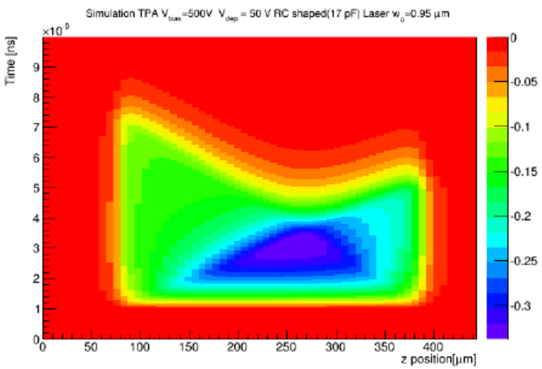

Simulation with TRACS

TRACS-Transient current simulator Simulates the shape of TCT techniques

[I. Vila, 25th RD50 workshop]
[R. Palomo, 25th RD50 workshop]
[P. Castro, 25th RD50 workshop]

Low Resistance Strip Sensors

- Coupling capacitors can get damage due to the beam loss since there is a large charge deposition.
- Deposition of Aluminum on top of the implant: $R_{\square}$(Al) ~ 0.04 W/□ ⇒ 20 W/cm (Drastic reduction of strip resistance!)
- Metal layer deposition on top of the implant (first metal) before the coupling capacitance is defined (second metal)

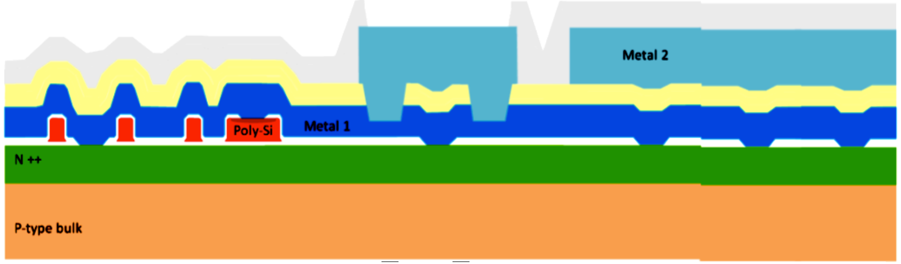

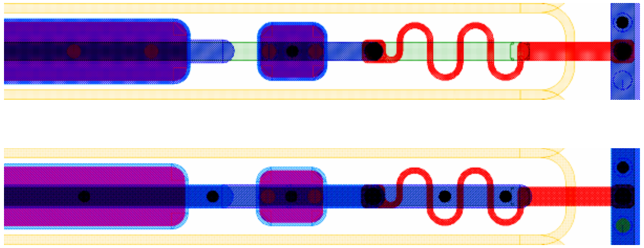

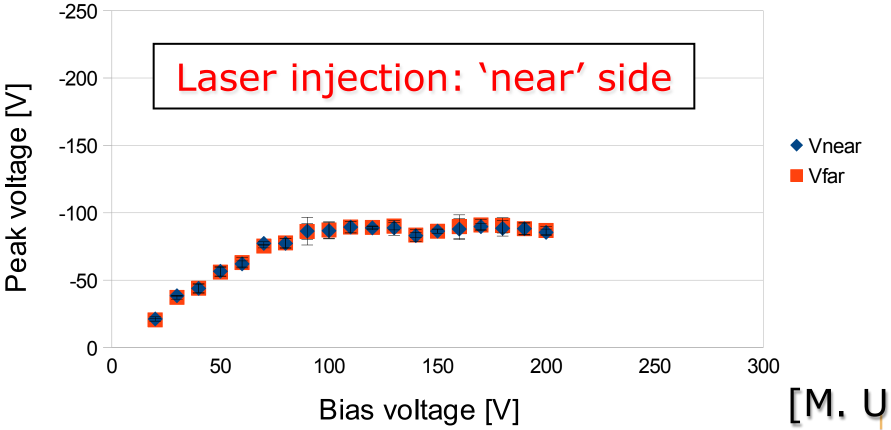

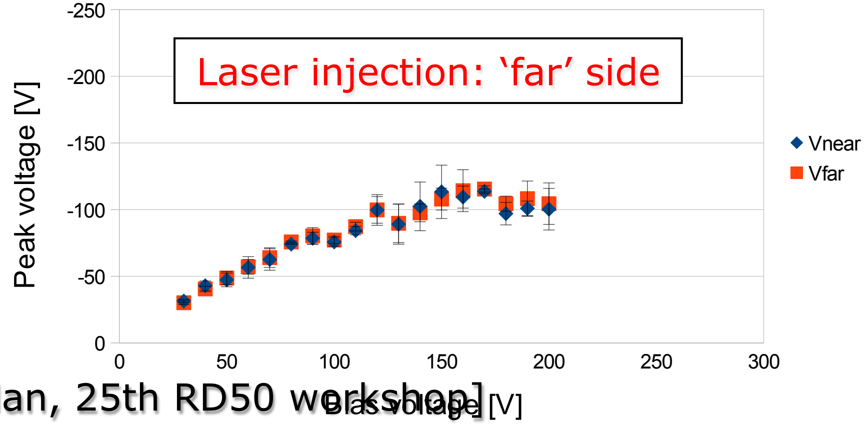

[M. Ullan, 25th RD50 workshop]